

## Mechanism of current leakage in Ni Schottky diodes on cubic GaN and $\text{Al}_x\text{Ga}_{1-x}\text{N}$ epilayers

D.J. As<sup>1</sup>, S. Potthast<sup>1</sup>, J. Fernandez<sup>1</sup>, K. Lischka<sup>1</sup>, H. Nagasawa<sup>2</sup>, M. Abe<sup>2</sup>

<sup>1</sup>University of Paderborn, Department of Physics, Warburger Str. 100, D-33098 Paderborn, Germany;

<sup>2</sup>HOYA Advanced Semiconductor Technologies Co., Ltd., 1-17-16 Tanashioda, Sagamihara, Kanagawa 229-1125, Japan

### ABSTRACT

Ni Schottky-diodes (SDs) 300  $\mu\text{m}$  in diameter were fabricated by thermal evaporation using contact lithography on cubic GaN and  $\text{Al}_x\text{Ga}_{1-x}\text{N}$  epilayers. Phase-pure cubic GaN and c- $\text{Al}_{0.3}\text{Ga}_{0.7}\text{N}/\text{GaN}$  structures were grown by plasma assisted molecular beam epitaxy (MBE) on 200  $\mu\text{m}$  thick free-standing 3C-SiC (100) substrates. The quality of the cubic group III-nitride epilayers was checked by high resolution X-ray diffractometry, atomic force microscopy and photoluminescence at room temperature and at 2 K. Large deviations from the thermionic emission transport were observed in the current voltage (I-V) behavior of these SDs. Detailed analysis of the I-V characteristics at 300 K and at low temperature showed that a thin surface barrier is formed at the Ni semiconductor interface. Thermal annealing in air at 200°C alters the composition of this thin surface barrier and reduces the leakage current by three orders of magnitude. The doping density dependence of breakdown voltages derived from the reverse breakdown voltage characteristics of c-GaN SDs is in good agreement with theoretically calculated values and follows the expected trend. From these experimental data a blocking voltage of higher than 600V is extrapolated for c-GaN films with a doping level of  $N_D = 5 \times 10^{15} \text{ cm}^{-3}$ .

### INTRODUCTION

In GaN-based electronic devices such as high-power high electron mobility transistors (HEMTs), high-power metal semiconductor field effect transistors (MESFETs) and UV-photodetectors Schottky contacts are key elements for realization [1]. For these devices the width of the Schottky contact depletion layer thickness has to be controlled precisely for optimum device operation. However, GaN based Schottky contacts suffer from abnormal large leakage currents under reverse bias [2], which strongly degrade gate control characteristics and increase power consumption. Different field emission (FE) models assuming a triangular Schottky potential [3], trap-assisted tunnelling [4], spatial variations of barrier heights [5] and the introduction of a thin surface barrier (TSB) [6] have been used to explain this leakage mechanism.

Cubic GaN, although more difficult to grow, allows a 50% gain in FET performance in comparison to wurtzite GaN as proposed by 2D Monte Carlo device simulations of nitrides field effect transistors (FET) [7]. If the cubic group-III nitrides are grown in (001) direction spontaneous and piezoelectric polarization effects can be avoided at the interfaces and surfaces.

The density of the two-dimensional electron gas (2-DEG) in cubic  $\text{Al}_x\text{Ga}_{1-x}\text{N}/\text{GaN}$  heterostructures will be independent on the thickness and Al mole fraction of the  $\text{Al}_x\text{Ga}_{1-x}\text{N}$  barrier layer and can be controlled by doping with silicon. The combination of these effects may be used to realize cubic  $\text{AlGaN}/\text{GaN}$  HEMTs with both normally on and normally off operation as it is strongly required from the system side for logic devices [8]. In addition the electronic structure of the cubic GaN (001) surface is different to that of the c-plane in hexagonal GaN and therefore may alters the electronic properties of the Schottky diodes [9].

In this work, we focus on the fabrication of cubic GaN (c-GaN) based Ni-Schottky-barrier devices (SBDs). The I-V characteristics are studied at different temperatures and the influence of thermal annealing in air at  $200^\circ\text{C}$  is investigated. The doping density dependence of breakdown voltages derived from the reverse breakdown voltage characteristics of c-GaN SBDs is investigated and from the experimental data the critical field for electronic breakdown in the cubic devices is determined.

## EXPERIMENTS

Phase-pure cubic GaN and  $\text{Al}_{0.3}\text{Ga}_{0.7}\text{N}/\text{GaN}$  structures were grown by plasma assisted molecular beam epitaxy (MBE) [10] on  $200\ \mu\text{m}$  thick free-standing 3C-SiC (100) substrates. The thickness of the c-GaN and c- $\text{Al}_{0.3}\text{Ga}_{0.7}\text{N}$  epilayers were about  $600\ \text{nm}$  and  $30\ \text{nm}$ , respectively. The quality of the cubic epilayers was checked by high resolution X-ray diffractometry, atomic force microscopy and photoluminescence. Details of the MBE growth of cubic GaN and on the properties of c-GaN on free standing 3C-SiC substrates are given elsewhere [11]. Ni/In ( $50\text{nm}/150\text{nm}$ ) Schottky contacts  $300\ \mu\text{m}$  in diameter were produced on c-GaN and c- $\text{Al}_{0.3}\text{Ga}_{0.7}\text{N}/\text{GaN}$  structures by thermal evaporation using contact lithography. Prior to vacuum deposition, the GaN and  $\text{Al}_{0.3}\text{Ga}_{0.7}\text{N}$  surfaces were cleaned by organic solvents and a buffered oxid etch (BOE). Pure In contacts were used for the ohmic contact to GaN or  $\text{Al}_{0.3}\text{Ga}_{0.7}\text{N}$  epilayers. A clear rectifying behavior was measured in our SBDs and the current voltage (I-V) behavior was studied in detail in the dark. Capacitance-voltage (C-V) measurements and electrochemical CV profiling (ECV) [12] were used to determine the net donor concentration in our cubic GaN and  $\text{Al}_{0.3}\text{Ga}_{0.7}\text{N}$  layers which varied between  $9 \times 10^{16}\ \text{cm}^{-3}$  to  $2 \times 10^{19}\ \text{cm}^{-3}$ .

## RESULTS AND DISCUSSION

In figure 1 the room temperature (RT) I-V curve (open circles) clearly demonstrates a rectifying characteristic for a typical Ni-Schottky contact on our as grown cubic GaN. In the inset a schematic drawing of the device structure is depicted. A net carrier concentration of  $N_D - N_A = 1.8 \times 10^{17}\ \text{cm}^{-3}$  is measured by C-V. From the linear increase of current with forward bias a series resistance of  $R_S = 230\ \Omega$  is obtained for the as grown sample. At  $-5\text{V}$  a reverse current of  $0.9\ \text{mA}$  is measured. By thermal annealing of the Ni contact at  $200^\circ\text{C}$  in ambient air the I-V characteristics improved severely as shown by the blue squares in figure 1. First a severe reduction

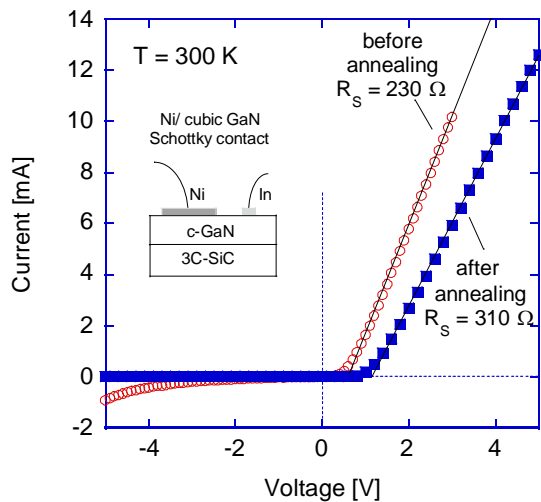


**Figure 1.** Room temperature current voltage ( $I$ - $V$ ) characteristics of a Ni-Schottky contact on cubic GaN before annealing (open circles) and after annealing in air at 200°C (full squares).

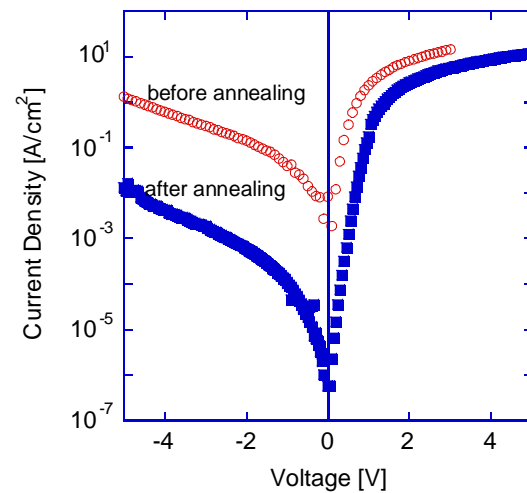


**Figure 2.** Semi-logarithmic plot of the  $I$ - $V$  characteristics of a Ni-Schottky contact on cubic GaN before annealing (open circles) and after annealing in air at 200°C (full squares).

of the reverse current to 0.00325 mA is measured at a bias of  $-5$  V and second an increase of the series resistance to  $R_s=310 \Omega$  is estimated. This dramatic improvement in the reverse current by about three orders of magnitude is emphasized in figure 2 in which the current bias dependence is plotted in a semi-logarithmic scale.

A detailed analysis of both the forwards  $I$ - $V$  characteristic as well as the reverse bias characteristic shows strong deviations from the standard thermionic emission (TE) model [13]. Whereas at RT the forward characteristic follows a thermionic emission (TE) model, the reverse bias dependence shows strong deviations, which are characterized by the following two salient features. First the magnitude of reverse current is generally larger (by orders of magnitude) than the reverse saturation current given by the TE model, and second a nearly exponential increase of the reverse current is observed at high reverse voltage (see Fig.2). This behavior is observed for both the as grown and the thermally annealed Schottky diodes.

To identify the mechanism responsible for this abnormal large leakage current temperature dependent  $I$ - $V$  measurements have been performed. Figure 3 shows the  $I$ - $V$  curves of the annealed samples at temperatures between 300 K and 50 K. One clearly sees that the experimental temperature dependence of the  $I$ - $V$  curves is surprisingly small in contrast to the behavior expected by pure thermionic emission. In the forward current characteristic one sees an indication of a current plateau in the low bias region as shown in the inset of figure 3. Such a plateau is a clear hint for the existence of serious tunneling transport [14]. An even stronger deviation from the expected thermionic behavior is seen in the reverse bias characteristic. The magnitude of the reverse current is nearly independent of the temperature and is orders of magnitude higher than that expected by

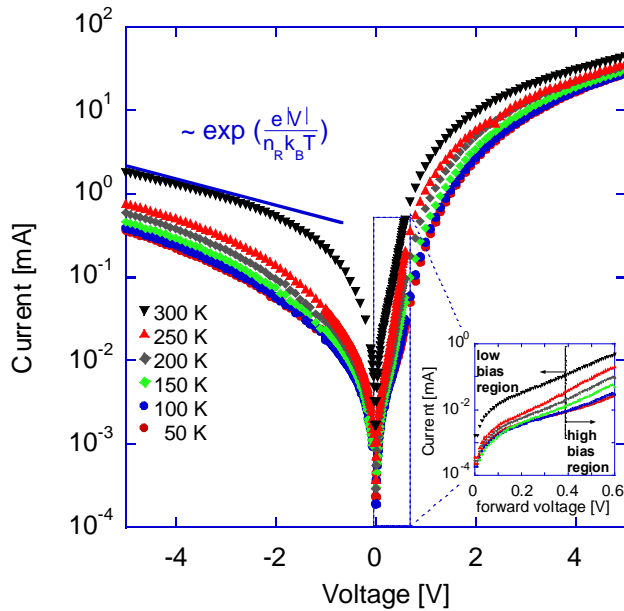


**Figure 3.** Current voltage ( $I$ - $V$ ) characteristics of the annealed Ni-Schottky contact on cubic GaN at temperatures between 300K and 50 K after annealing in air at 200°C (full squares). The inset emphasizes the formation of a current plateau in the low forward bias region.

therefore reduce the density of these  $V_N$  defects and improve the  $I$ - $V$  characteristic, which is in agreement with our experimental results. The influence of O may be more severe for  $Al_xGa_{1-x}N$  epilayers due to the increased affinity of Al to O. This is also in agreement to our observation that the leakage current is higher in  $Al_xGa_{1-x}N$  Schottky diodes than in GaN Schottky diodes (not shown here). Guo et al. [17] proposed that the formation of  $Ga_4Ni_3$ ,  $Ni_3N$  and  $Ni_4N$  at the Ni GaN interface during annealing at temperatures above 200°C is responsible for the reduction of the leakage current. These clusters may form defects, which may compensate the donor defects responsible for the formation of the TSB.

In figure 4 the reverse bias characteristics of three different Ni/GaN Schottky diodes are depicted. As expected the breakdown voltage ( $V_{Br}$ ) decreases with increasing carrier concentration for the as grown samples (open blue squares and open red circles). However, for the annealed sample (full green triangles) the breakdown voltage is higher even at a higher carrier concentration. A striking feature is that for all samples breakdown occurs at the same current density of about  $200 A/cm^2$ . Whereas for the as grown samples the reverse bias characteristic can be described by one single exponential relationship the slopes for the annealed samples clearly consist of at least two, one for low reverse bias and one for high reverse bias. This exponential relationship can well be explained by the TSB model and indicates that by the thermal annealing

the TE model, especially at the lower temperatures. The reverse current shows a strong dependence on the voltage, which can be roughly described by an exponential relationship (see full straight line and the corresponding formula in figure 3).

Recently, Hasegawa et al. [15] observed similar features with Ni, Pt and Au Schottky contacts in hexagonal GaN (h-GaN), which they explained by introducing a thin surface barrier (TSB) model. This TSB model proposes the formation of a highly conductive layer due to the presence of defect donors at the interface between the Ni metal and GaN epilayer. In this case the TSB reduces the barrier thickness and allows severe tunneling of free carriers (field emission). For GaN and  $Al_xGa_{1-x}N$  nitrogen vacancies ( $V_N$ ) or oxygen impurities ( $O_N$ ) are proposed to be the reason for this donor defects [16]. Thermal annealing in air or nitrogen may

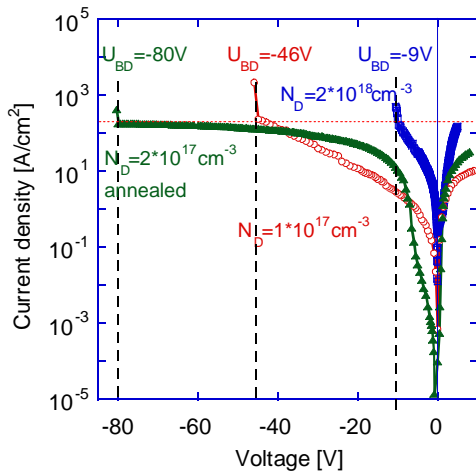


**Figure 4.** Semilogarithmic plot of the  $I$ - $V$  characteristic of Ni-Schottky contacts with different doping concentration on cubic GaN.

the properties of the thin surface barrier are changed. Detailed analysis of this behavior is under way and will be published elsewhere.

One of the most significant parameters in the design and performance of high power devices is the critical field of electric breakdown, which can be estimated from the measured breakdown voltage of SBDs. For hexagonal GaN breakdown voltages of up to 450V and 550 V have been reported for about 10  $\mu\text{m}$  thick HVPE grown [18] and 3 $\mu\text{m}$  thick MOCVD grown [19] epilayers, respectively. However, due to the presence of defects like dislocations, nanopipes or voids premature breakdown in hexagonal GaN has been measured. In cubic group III-nitrides nanopipes or voids have never been observed, however the density of dislocations is in the same order of magnitude, about  $10^{10}\text{cm}^{-2}$ , as in the hexagonal case. Figure 5 shows

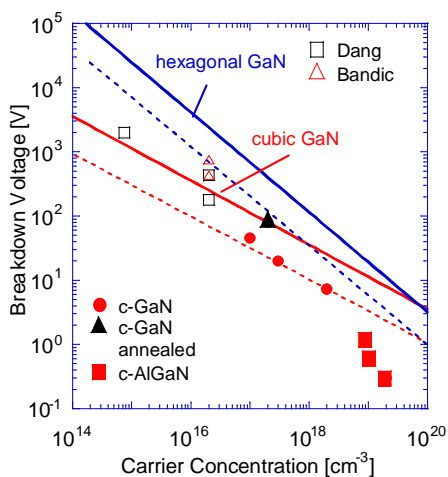


**Figure 5.** Reverse breakdown voltage versus carrier concentration.

the breakdown voltages derived from the reverse breakdown voltage characteristic of c-GaN SDs as a function of the doping density ( $N_D - N_A$ ), which was measured either by C-V or ECV. The experimental data (full red circles) are in good agreement with theoretically calculated values [20] depicted in figure 5 by the full lines for both c-GaN (red) and h-GaN (blue). From these experimental data a critical electric field of about  $E_{\text{crit}} \approx 2.3 \times 10^6 \text{V/cm}$  is determined and a blocking voltage of higher than 600V is extrapolated for c-GaN films with  $N_D = 5 \times 10^{15} \text{cm}^{-3}$ . Included in figure 5 are also experimental data obtained on h-GaN (open squares [19] and open triangles [18]). The experimental values of  $V_{\text{Br}}$  in c-GaN are one-third smaller than the theoretical values and show the same dependence on doping level as in h-GaN (dashed lines). Crystal defects like dislocations or point defects may be the reason for the deviation between experimental data and theoretical calculations. This interpretation is supported by the experimental data obtained on the annealed sample (full triangle), where the measured  $V_{\text{Br}}$  of 80 V at a carrier concentration of  $1.8 \times 10^{17} \text{cm}^{-3}$  is in excellent agreement with the theoretical curve. For c- $\text{Al}_{0.3}\text{Ga}_{0.7}\text{N}$  epilayers (full squares) the larger deviation to the theoretical curve may be a hint for the existence of a more pronounced TSB due to a higher  $\text{O}_\text{N}$  concentration.

## CONCLUSIONS

Ni Schottky-barrier devices were fabricated by thermal evaporation using contact lithography on cubic GaN and  $\text{Al}_x\text{Ga}_{1-x}\text{N}$  epilayers. Phase-pure cubic GaN and c- $\text{Al}_{0.3}\text{Ga}_{0.7}\text{N}/\text{GaN}$  structures were grown by plasma assisted MBE on 200  $\mu\text{m}$  thick free-standing 3C-SiC substrates. Analysis of the I-V characteristic of these SBDs at 300 K and at low temperature showed that a thin surface barrier is formed at the Ni GaN interface. Thermal annealing in air at 200°C alters this thin surface barrier and reduces the leakage current by three orders of magnitude. The doping density dependence of  $V_{\text{Br}}$  is in good agreement with calculated values and follows the expected trend. From these experimental data a critical electric field of about  $E_{\text{crit}} \cong 2.3 \times 10^6 \text{V/cm}$  is determined.

## REFERENCES

1. H. Morkoc and L. Liu, "GaN-based modulation-doped FETs and heterojunction bipolar transistors", in edited by P. Ruterana, M. Albrecht and J. Neugebauer, (WILEY-VCH Verlag GmbH, 2003) pp.547
2. V. Adivarahan, G. Simin, J.W. Yang, A. Lunev, M. Asif Khan, N. Pala, M. Shur and R. Gaska, *Appl. Phys. Lett.* **77** (6), 863 (2000).
3. E.J. Miller, X.Z. Dang and J. Yu, *J. Appl. Phys.* **88** (10), 5951 (2000).
4. S. Karmalkar, D.M. Sathaiya and M.S. Shur, *Appl. Phys. Lett.* **82** (22), 3976 (2003).
5. S. Chand and S. Bala, *Appl. Surf. Sci.* **252**, 358 (2005).
6. S. Kotani, T. Hashizume and H. Hasegawa, *J. Vac. Sci. Technol. B* **22** (4), 2179 (2004).
7. F. Dessenne, D. Cichocka, P. Desplanques and R. Fauquembergue, *Mat. Sci. and Eng. B* **50**, 315 (1997).
8. M. Abe, H. Nagasawa, S. Potthast, J. Fernandez, J. Schörmann, D.J. As and K. Lischka, *IEICE Transaction on Electronics*, will be published in July (2006).
9. T. Maxisch and A. Baldereschi, *phys. stat. sol. (c)* **2** (7), 2540 (2005).
10. D.J. As, "Growth and characterization of MBE-grown cubic GaN,  $\text{In}_x\text{Ga}_{1-x}\text{N}$ , and  $\text{Al}_y\text{Ga}_{1-y}\text{N}$ ", in *Optoelectronic Properties of Semiconductors and Superlattices*, Vol. **19**, edited by M.O. Manasreh and I.T. Ferguson, (Taylor & Francis Books, Inc., 2003) pp.323
11. D.J. As, S. Potthast, J. Schörmann, S.F. Li, K. Lischka, H. Nagasawa and M. Abe, *Proc. of ICSCRM (Pittsburgh)*, FA2. EPI IV p.82 Sept. (2005).
12. T. Wolff, M. Rapp and T. Rotter, *phys. stat. sol. (c)* **1** (10), 2491 (2004).
13. D.K. Schroder, in *Semiconductor Material and Device Characterization*, Wiley and Sons, New York (1990)
14. D. Donoval, M. Barus and M. Zdimal, *Solid State Electronics* **34** (12), 1365 (1991).
15. H. Hasegawa and S. Oyama, *J. Vac. Sci. Technol. B* **20** (4), 1647 (2002).
16. S. Oyama, T. Hashizume and H. Hasegawa, *Appl. Surf. Sci.* **190**, 322 (2002).
17. J.D. Guo, F.M. Pan, M.S. Feng, R.J. Guo, P.F. Chou and C.Y. Chang, *J. Appl. Phys.* **80** (3), 1623 (1996).
18. Z.Z. Bandic, P.M. Bridger, E.C. Piquette and T.C. McGill, *Appl. Phys. Lett.* **74** (9), 1266 (1999).
19. G.T. Dang, A.P. Zhang, M.M. Mshewa, F. Ren, J.I. Chyi, C.M. Lee, C.C. Chuo, G.C. Chi, J. Han, S.N.G. Chu, R.G. Wilson, X.A. Cao and S.J. Pearton, *J. Vac. Sci. Technol. A* **18** (4), 1135 (2000).
20. K. Matocha, T.P. Chow and R.J. Gutmann, *Materials Science Forum* **383-393**, 1531 (2002).